Design of an Electronic Air Cleaner with Porous Collecting Electrodes

Igor Krichtafovitch, Tsrong-Yi Wen, and Alexander V. Mamishev

Department of Electrical Engineering, University of Washington
phone: (206) 221-5729
e-mail: mamishev@uw.edu

***Abstract* — A novel electronic air cleaner (EAC) was built, consisting of a fan and a series of electrodes, including corona electrodes, repelling electrodes, and collecting electrodes. The collecting electrodes were covered with foam. Due to the foam's porous structure and weak electrical conductivity, the foam reduces the chance of spark discharging and of particulates re-entering the environment, both of which happen frequently in traditional EAC systems. This study presents a technical background on the underlying principles of electrohydrodynamics (EHD) used in EAC systems. This study also presents a comprehensive discussion on the design concepts and schematics of the new EAC system. Experimental results indicate that the filtration efficiency of the new EAC system is above 99%. The filtration efficiency is affected by the voltage at both the corona and repelling electrodes.**

I. INTRODUCTION

Traditional electrostatic precipitators (ESPs), also known as electronic air cleaners (EACs), have several drawbacks: 1) filtration efficiency depends on the dust conductivity and amount of dust collected, 2) accumulated dust and chemical contamination decreases the corona electrode's ability to generate ions, 3) poor particle adherence to collecting electrodes lead to particulates re-entering the environment, and 4) frequent sparking and arc discharging decreases filtration efficiency.

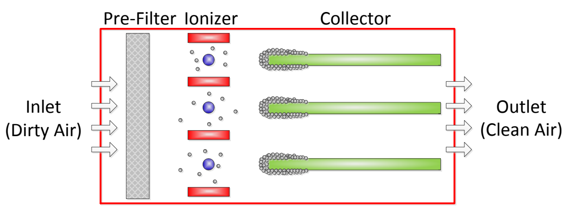

Fig. 1. Schematics of a traditional three stages EAC system.

A schematic diagram of the traditional three stages EAC system is shown in Fig. 1. The inlet air is drawn into the system by a fan and is filtered by a pre-filter. Then, it is ionized via the ionizer, such that ionized molecules and particles collide with and attach to the neutral molecules and particles (i.e., charging them). As those charged particles pass through a set of electrode plates, they are repelled and attach to the collecting electrodes because of a strong electric field between the repelling and collecting electrodes. As a result, the particles in the air are removed and the remaining outlet air is clean.

The key feature of the new EAC system is that the collecting electrodes are covered with a porous material that has weak electrical conductivity. This foam structure provides some benefits. First, the porous surface is capable of accumulating a significantly greater amount of dust without compromising filter performance. The dust penetrates deep into the holes, leaving the collecting electrode surface nearly clean for a long duration, and sharply eliminating the chance of particulates re-entering the environment. Second, the weak electrical conductivity of the foam prevents spark discharging between the electrodes. This feature is important because when spark discharging occurs between the electrodes, it can be considered a short circuit, which means that there is no electric field between the electrodes; in other words, the filter does not work when spark discharging occurs. Therefore, the weak electrical conductivity of the foam allows us to remove the inlet pre-filter (mandatory in conventional EACs, as shown in Fig. 1), which is used for short-circuit prevention. The weak electrical conductivity of the foam also keeps conductive dust from fast discharging and re-entering the environment. Third, the foam is flame retardant, thus it would not start or support a fire.

II. IMPLEMENTATION

A. Technical Background

The physical principles of an EAC are based on electrohydrodynamics (EHD), which are the behaviors that involve fluid dynamics, electrostatics, and charge transport. For a positive discharging model, as shown in Fig. 2, the corona electrode operates at high positive voltage and the collecting electrode is usually grounded, hence there is a high intensity electric field between the corona and collecting electrodes. The particles or molecules surrounding the corona electrode are ionized. These ionized particles or molecules are repelled against the corona electrode, and then travel toward the collecting electrode in accordance with the electric field, and finally, settle down on the collecting electrode.

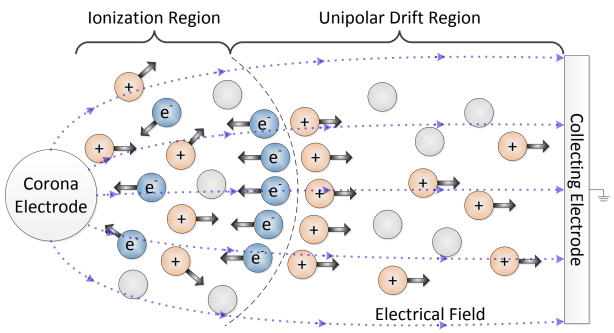

Fig. 2. Model of positive discharging. There are two regions between the corona and collecting electrodes. The ionization region, or corona plasma region, is formed and surrounds the corona electrode. The drift region is the region between the ionization boundary and the collecting electrode.

As shown in Fig. 2, there are two regions in between the corona and collecting electrodes: the ionization region and the unipolar drift region. The ionization region exists very close to the corona electrode, and there are both positive and negative ions inside this region. Because the radius of the corona electrode is much smaller than the distance between the corona and collector electrodes, the radius of the ionization region can be evaluated by Peek's law [1] and Kaptsov's assumption [2-4], where Peek's law is to estimate the electric field at the corona electrode surface, while Kaptsov's assumption states that the electric field at the ionization boundary equals the breakdown voltage of the fluid which, in this case, is air. Equation (1) shows how to get an electric field at the corona electrode surface by a given radius of the corona electrode, whereas (2) gives the radius of the ionization region in terms of the radius of the corona electrode.

$$E_w = E_0\left(1+\frac{2.62\times10^{-2}}{\sqrt{R_w}}\right) \tag{1}$$

$$R_0 = R_w\left(1+\frac{2.62\times10^{-2}}{\sqrt{R_w}}\right) \tag{2}$$

where E_w is the electric field strength at the corona electrode surface, E_0 is the breakdown electric field strength of air, R_0 is the radius of the ionization region, and R_w is the corona electrode radius.

The other region is the unipolar drift region, where the ionized particles or molecules travel toward the collecting electrode. Within this region, the moving particles obey classical fluid dynamics, which is represented by Navier-Stoke's equation, as shown in (3). The body force in Navier-Stoke's equation comes from the Coulomb force [5, 6], which is the result of electrostatic interactions between charged particles, as shown in (4).

$$\rho\mathbf{U}\cdot\nabla\mathbf{U} = -\nabla p + \mu\nabla^2\mathbf{U} + \mathbf{f} \tag{3}$$

$$\mathbf{f} = -q\nabla V \tag{4}$$

where ρ is fluid density, $\mathbf{U}$ is velocity field, p is fluid pressure, μ is fluid dynamic viscosity, $\mathbf{f}$ is body force, q is charge density, and V is electric potential.

B. Prototype Design Concept and Realization

The main problem of traditional EACs is that it is not easy to stick accumulated dust tightly onto the collecting electrodes. Vibration or passing airflow causes the accumulated dust to return to the environment. Therefore, the key feature of the new EACs is that we attach foam to the collecting electrode. Fig. 3 is the schematic diagram of the new EAC.

A traditional fan is used to draw certain amounts of air into the device. When the air travels through the corona electrodes, the particles in the air are charged due to the ionization process. As these ionized particles move forward, they will experience a high intensity electric field and be impelled toward the collecting electrodes. Due to the collecting foam, which is a porous and semi-conductive material, the particles will fall into the porous holes and will not easily return to the environment. The semi-conductive property gives two benefits: 1) ensuring that the foam does not decrease the electric field intensity between the repelling and collecting electrodes, and 2) preventing discharging or sparking due to any highly-curved geometry.

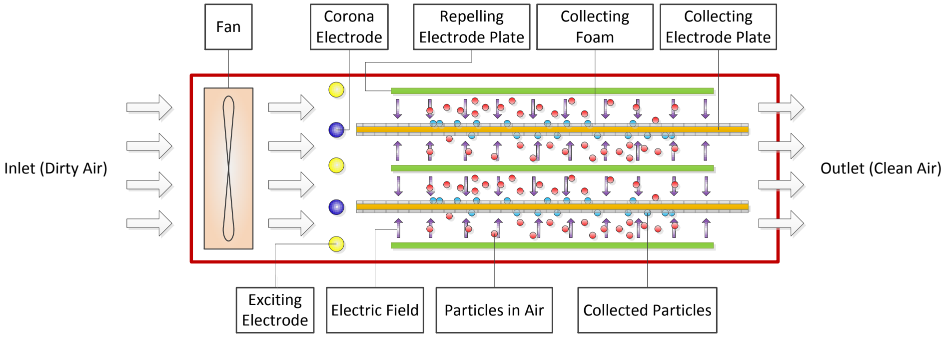

Fig. 3. Schematic diagram of the EAC with porous foam on the collecting electrodes.

The prototype of the new EAC is built with the enclosure dimension of approximate eight inches by eight inches by five inches, and it is made with rigid plastic. The collecting electrodes and the repelling electrodes are arranged periodically. Both sides of the collecting electrodes are covered with foam. Fig. 4 shows the CAD outline of the new EAC.

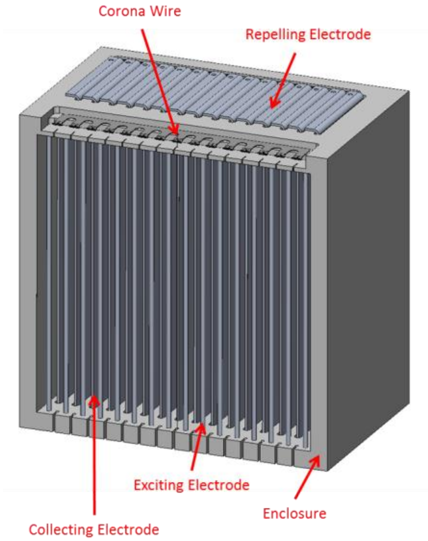

Fig. 4. Outline of the prototype of the new EAC.

III. Measurements of filtration efficiency

A. Configuration

Fig. 5 demonstrates the testing setup. The air is drawn by four fans. Then, the air runs through a stabilizer to ensure uniform airflow. The air velocity is variable by adjusting the input voltage. All air travels toward the new EAC prototype. The particle counter, placed right after the EAC prototype, is used to measure how many particles are in the air, in the catalog of particle size.

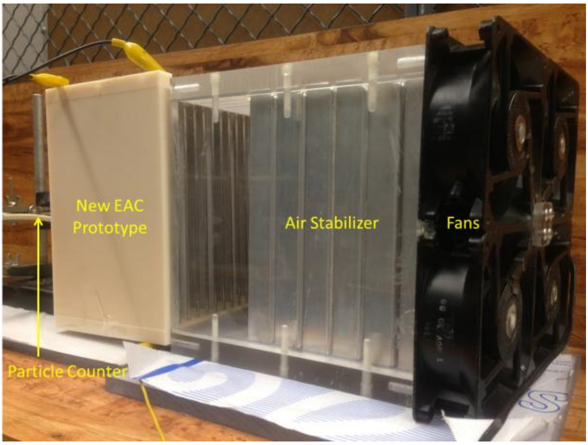

Fig. 5. Testing setup, including fans, air stabilizer, new EAC prototype, and particle counter.

B. Filtration Efficiency

We measured the number of particles at various corona electrode voltages. The voltage of the repelling electrode was kept at 15 kV and the collecting electrode was grounded. The air velocity was maintained at 500 ft/min. The particle counter was used to measure particles with 0.3 um to 0.5 um in diameter. The number of background particles (i.e., the number of particles when the EAC is off) was, on average, 668. Table 1 shows the number of detected particles and corresponding filtration efficiency, while Fig. 6 demonstrates both filtration efficiency and power consumption of the EAC itself (fan power is not accounted for). The number of detected particles decreases quickly when the voltage of the corona electrode increases. This can be explained in the following way: the particles are not charged enough when the voltage of the corona electrode is low, and therefore, more particles are detected by the particle counter than when the voltage of the corona electrode is sufficiently high. At a corona voltage of 4.5 kV, the filtration efficiency is 99%, and the corresponding energy consumption of the EAC itself is 6.8 watts. Note that power consumption is ignorable between repelling and collecting electrodes because the current across them is almost zero.

Table 1. Particle detected and corresponding filtration efficiency at different corona voltages. There were 668 background particles.

Voltage at Corona Electrodes (kV)	Detected Particles	Filtration Efficiency (%)
4.0	103	84.56
4.1	35	94.76
4.2	10	98.50
4.3	19	97.16
4.5	7	98.95
4.6	5	99.25
4.8	6	99.10

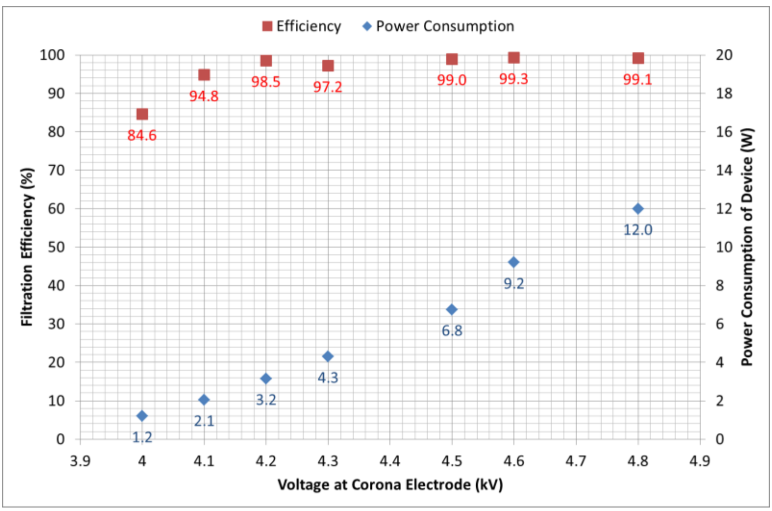

Fig. 6. Measurements of the filtration efficiency and the power consumption of the EAC itself at different corona electrode voltages. The particle diameter we focused on was 0.3 um to 5.0 um. The air velocity was 500 ft/min. The voltage at repelling electrode was 15 kV.

We measured the number of particles with various repelling voltages as well. The air velocity was, again, 500 ft/min. The corona wire voltage was kept at 5 kV. Fig. 7 shows the filtration efficiency based on 668 background particles. The filtration efficiency is greater than 97% when the repelling voltage is greater than 11 kV. The efficiency increases when the electric field strength is stronger, which is expected since stronger electric fields can push charged particles faster toward the collecting electrode because the resultant force toward the collecting electrode is also stronger, as demonstrated in Fig. 8.

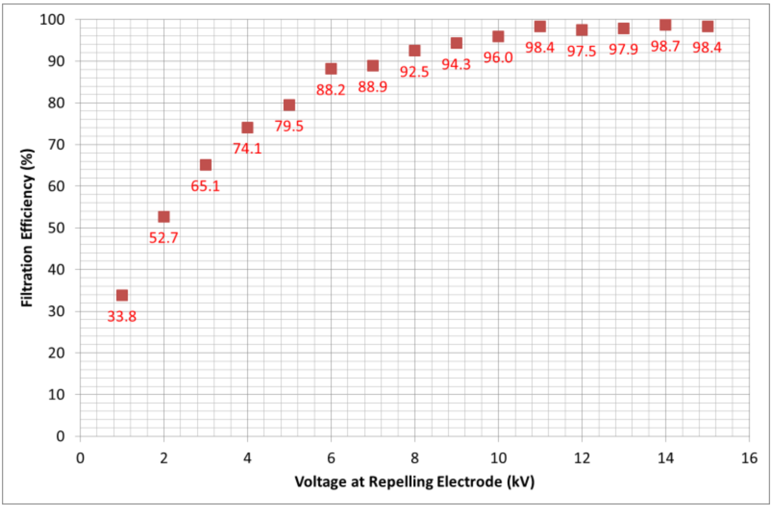

Fig. 7. Measurements of the filtration efficiency at different repelling electrode voltages. The particle diameter we focused on was 0.3 to 5.0 micrometers. The air velocity was 500 ft/min. The voltage at the corona electrode was 5 kV.

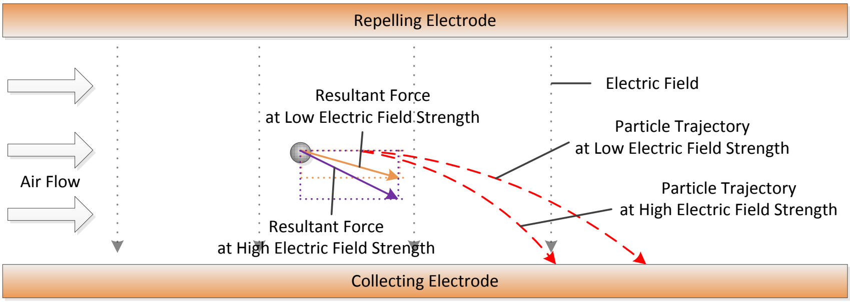

Fig. 8. Particle trajectories with high and low electric field strength. Not drawn to scale.

IV. Conclusion

One of the critical concerns of traditional EACs is that particulates return to the environment because of reasons like vibration or strong airflow. For the new EAC, porous foam is attached to the collecting electrodes to address the concern of particulates re-entering the environment. The weak electrical conductivity of the foam can prevent sparking and discharging between repelling and collecting electrodes, which ensures that the electric field in between is continuously working. On the other hand, the weak electrical conductivity of the foam does not decrease the electric field strength between the repelling and collecting electrodes.

Through testing, we know that voltage at the corona electrodes influences both filtration efficiency and power consumption. Higher voltage at the corona electrode can sufficiently charge particles and result in higher filtration efficiency. However, power consumption and filtration efficiency are not linearly dependent on each other. Our results suggest that it is not necessary for the voltage at the corona electrode to be as high as possible since the filtration efficiency is high enough at a certain high voltage. For the new EAC, 4.5 kV at the corona electrode results in 99% filtration efficiency and only consumes 6.8 watts.

Additionally, voltage at the repelling electrodes has more influence on the filtration efficiency than at the corona electrode since voltage at the repelling electrodes determines the electric field strength between the repelling and collecting electrodes. For the new EAC, the filtration efficiency gradually increases from 33% to 98%, where the filtration efficiency can be nearly saturated at 11 kV repelling voltage.

REFERENCES

[1] F. W. Peek, *Dielectric phenomena in high voltage engineering*: McGraw-Hill, 1929.

[2] N. A. Kaptsov, "*Elektricheskie Yavvleniya Gazakh i Vakuume*," 1947.

[3] K. Adamiak and P. Atten, "Simulation of corona discharge in point–plane configuration " *Journal of Electrostatics*, vol. 61, pp. 85-98, 2004.

[4] M. Quast and N. R. Lalic, "Measuring and Calculation of Positive Corona Currents Using Comsol Multiphysics " *Proceedings of the COMSOL Conference*, 2009.

[5] H. C. Chang and L. Y. Yeo, *Electrokinetically driven microfluidics and nanofluidics*: Cambridge University Press, 2010.

[6] B. Komeili, J. S. Chang, G. D. Harvel, C. Y. Ching, and D. Brocilo, "Flow characteristics of wire-rod type electrohydrodynamic gas pump under negative corona operations," *Journal of Electrostatics*, vol. 66, pp. 342-353, 2008.